Published in final edited form as:
Reprod Toxicol. 2014 January ; 43: 111–124. doi:10.1016/j.reprotox.2013.12.002.

Eye-Specific Gene Expression following Embryonic Ethanol Exposure in Zebrafish: Roles for Heat Shock Factor 1

Bhavani Kashyap[a,b], **Laurel Pegorsch**[a], **Ruth A. Frey**[a], **Chi Sun**[a,b], **Eric A. Shelden**[c,d], and **Deborah L. Stenkamp**[a,b,d,*]

[a]Department of Biological Sciences, University of Idaho, Moscow, ID 83844

[b]Neuroscience Graduate Program, University of Idaho, Moscow, ID 83844

[c]School of Molecular Biosciences, Washington State University, Pullman WA 99164

[d]Center for Reproductive Biology, University of Idaho, Moscow, ID 83844

Abstract

The mechanisms through which ethanol exposure results in developmental defects remain unclear. We used the zebrafish model to elucidate eye-specific mechanisms that underlie ethanol-mediated microphthalmia (reduced eye size), through time-series microarray analysis of gene expression within eyes of embryos exposed to 1.5% ethanol. 62 genes were differentially expressed (DE) in ethanol-treated as compared to control eyes sampled during retinal neurogenesis (24-48 hours post-fertilization). The EDGE (extraction of differential gene expression) algorithm identified >3000 genes DE over developmental time in ethanol-exposed eyes as compared to controls. The DE lists included several genes indicating a mis-regulated cellular stress response due to ethanol exposure. Combined treatment with sub-threshold levels of ethanol and a morpholino targeting *heat shock factor 1* mRNA resulted in microphthalmia, suggesting convergent molecular pathways. Thermal preconditioning partially prevented ethanol-mediated microphthalmia while maintaining Hsf-1 expression. These data suggest roles for reduced Hsf-1 in mediating microphthalmic effects of embryonic ethanol exposure.

Keywords

Ethanol; Fetal Alcohol Syndrome; Eye; Microarray; Zebrafish; Heat Shock Factor; Heat Shock Protein; Retina

1. Introduction

Maternal alcohol consumption during human pregnancy results in a spectrum of defects in the fetus termed Fetal Alcohol Spectrum Disorder (FASD). The most severe form of FASD, fetal alcohol syndrome (FAS) is characterized by growth abnormalities, cardiac defects, and

*Author for correspondence: Deborah L. Stenkamp, Ph.D., Professor, Biological Sciences, University of Idaho, Moscow, ID 83844-3015, dstenkam@uidaho.edu.

Conflict of Interest Statement: The authors (Bhavani Kashyap, Laurel Pegorsch, Ruth Frey, Sun Chi, Eric Shelden, and Deborah Stenkamp) of "Eye-specific gene expression following embryonic ethanol exposure in zebrafish: Roles for heat shock factor 1," declare no conflicts of interest.

nervous system deficits, as well as ocular problems that persist postnatally [1]. Children with FAS show a variety of ocular defects ranging from major defects such as microphthalmia, coloboma of iris, and optic nerve hypoplasia, to minor visual impairment including reduced visual acuity and reduced contrast sensitivity [2]. Ocular manifestations are seen in 90% of children with FAS [3].

It is still unclear how ethanol targets different developing organ systems. Animal models provide a useful means to study targeted pathogenesis of FAS, as the defects can be replicated in developing mice, chick, *Xenopus* and zebrafish exposed to ethanol. For example, effects of ethanol on the Sonic hedgehog (Shh) signaling pathway [4], and strain-specific effects of ethanol upon global gene expression patterns within embryonic headfold tissue [5] were demonstrated using mouse models. Zebrafish, with their numerous advantages (large numbers, rapid external development, genetic tools) have recently become a popular model for studying the effects of ethanol. Most manifestations of FAS can be replicated in zebrafish, including cyclopia [6, 7]; microphthalmia with retinal abnormalities [8-14]; axial defects [15, 16] and neurobehavioral defects [17, 18]. In addition, similar to the situation in mouse, these effects are strain-dependent [19].

There is evidence from numerous animal models, including the zebrafish, that the axial defects of embryonic ethanol exposure are at least in part mediated by changes in retinoic acid (RA) signaling [20-22] or by changes in Shh signaling [23-25]. We recently tested these two candidate mechanisms for roles in mediating the microphthalmic effects of ethanol in zebrafish, specifically when ethanol was administered during the period of retinal neurogenesis [13]. In this study, RA treatments did not rescue the microphthalmic phenotype, and RA signaling was not reduced in the eye as a consequence of ethanol treatment [13]. In addition, exogenous cholesterol (required for Shh protein processing [26]) did not rescue the small eye phenotype of embryos treated with ethanol over the time of retinal neurogenesis, and the expression of *shh*, and of *ptc-2*, which is regulated by the Shh signaling pathway [27], were not altered in ethanol-induced microphthalmia in zebrafish eye tissues [13]. Hence, it remains unclear how ethanol exerts its teratogenic effects upon the eye during retinal neurogenesis.

Microarray studies have the potential to identify gene expression patterns that contribute to disease development and progression. Previous studies in mouse whole embryo and fetal brain tissue [5, 28-32] using a single time point microarray approach yielded a set of genes (and micro-RNAs) with diverse biological functions differentially expressed in ethanol-treated animals. The time series microarray approach is becoming an increasingly popular method for gene expression studies, particularly during development [33], tissue regeneration [34], in response to environmental stressors [35], in applications for which independent sampling schemes are used [36] and when sample numbers are limited [37, 38].

Here we present a time series microarray analysis of eye-specific gene expression during ethanol exposure in the zebrafish as an unbiased approach for discovery of mechanisms underlying the microphthalmic effects of ethanol. We exposed embryos to ethanol during retinal neurogenesis (24-48 hours post-fertilization; hpf), using an ethanol exposure (1.5%) that results in tissue ethanol concentrations similar to those measured in humans following 2-3 alcoholic drinks [13, 24]. We identified components of the cellular stress (“heat shock”) response as differentially expressed over time in eyes of ethanol-exposed embryos, and then tested the hypothesis that the cellular stress response is a critical target for ethanol toxicity in the eye through gene expression studies and functional analyses. The mRNA and protein corresponding to Heat shock factor 1 (Hsf-1), a transcriptional regulator of the heat shock response [39] were reduced in eyes of ethanol-treated embryos, and combined treatment of embryos with sub-threshold levels of ethanol and of an antisense morpholino (MO) targeting

hsf-1 resulted in significant microphthalmia. Thermal preconditioning induced expression of *hsp-70*, an Hsf-1 target [40], maintained Hsf-1 expression, and partially prevented microphthalmia in ethanol-treated embryos. These results are consistent with a working model whereby mis-regulation of Hsf-1 and Hsp-70 mediates the microphthalmic effects of embryonic ethanol exposure in zebrafish.

2. Material and Methods

2.1 Animals, Ethanol Treatments and Tissue Processing

Adult zebrafish were maintained in a light:dark (14:10 hour) cycle in our in-house, recirculating zebrafish facility at 28.5°C [41]. All animal use was approved by the University of Idaho Animal and Care Use Committee. Zebrafish were from a strain originally obtained from Scientific Hatcheries (SciH, now Aquatica BioTech; Sun City Center, FL) and maintained in-house. Adult zebrafish were bred, embryos were collected and placed in beakers with system water at 28.5°C.

Embryos were exposed to 1.5% ethanol as in Kashyap et al., 2007 [8]. Briefly, embryos, still within their chorions, were added to a 1.5% ethanol solution (diluted from 100% ethanol with system water) in glass beakers, and beakers were loosely covered with parafilm to reduce evaporation. This ethanol exposure results in significant microphthalmia (reduced eye size), and several accompanying retinal and lens abnormalities [8]. All ethanol exposures (Supplemental Table 1) took place beginning at 24 hpf.

For histological analysis, embryos were fixed with 4% paraformaldehyde in phosphate-buffered (pH 7.4) 5% sucrose, followed by a series of washes with increasing concentrations of sucrose [42]. Embryos were cryoprotected in buffered 20% sucrose overnight and were embedded in OCT embedding medium (Sakura Finetek, Torrance, CA) with 20% sucrose-phosphate buffer (1:2) by immersion in liquid N_2-cooled isopentane. Frozen blocks were sectioned at 5μm using a cryostat.

For extraction of eye-specific RNA, ethanol-treated and control embryos were collected at 24, 27, 30, 36, and 48 hpf (Supplemental Table 1), and were fixed using a methanol fixation procedure [43]. This procedure preserves the embryo biochemically and allows the embryo to be firm enough for dissection. Eyes were dissected from the rest of the body using curved, sharpened forceps and minutien pins. The bodies and eyes were refrozen separately for extraction of total RNA.

2.2 Microarray and Analysis

Total eye-specific RNA (20ng/μl; 5μl) was extracted from 50 embryos (100 eyes in each experimental sample) using the RNeasy mini kit (Qiagen) for both control (24, 27, 30, 36, and 48 hpf) and 1.5% ethanol-treated (27, 30, 36, 48 hpf) embryos (Supplemental Table 1). RNA was quantified using a Nano-Drop 1000 (Thermo-Scientific, Wilmington, DE), and RNA quality was verified using the Agilent Bioanalyzer (Agilent Technologies, Inc, Wilmington, DE). Total RNA was amplified using the NuGen kit (San Carlos, CA). Gene expression in eye-specific samples was determined using Affymetrix GeneChip Zebrafish Genome Arrays (Affymetrix, Santa Clara, CA). Microarray procedures were performed at the Genomics Core of the Center for Reproductive Biology, Washington State University (Pullman, WA).

The raw data from the probes of the microarray chips were adjusted for background, normalized, and presented as RMA (Robust Multi-array Average) using the Bioconductor package in the R statistical environment. Two approaches were used to identify differentially expressed genes: 1) *SAM (significance analysis of microarray) analysis* [36],

to detect genes that are differentially expressed in control as compared to ethanol treated embryo eyes using data representing all sampling times, and 2) *EDGE (Extraction of differential gene expression) algorithm* [44], a statistical approach to identify genes that are differentially expressed over time in control vs. ethanol-treated embryo eyes. A gene ontology (GO) analysis was performed using a web based tool, GOEAST [45], to identify relevant biological processes overrepresented in the differentially expressed gene sets obtained using the EDGE2 approach. GO categories were also used as filters to generate lists and/or heatmaps of differentially expressed genes within specific categories. Average-linkage, hierarchical clustering was performed using EDGE software, in the R programming environment. Clusters were built using mean-centered data, and with the correlation distance option, similar to the approach of [46], and displayed using the heatmap function.

2.3 Quantitative-RT-PCR (qRT-PCR)

2.3.1 Eye-specific gene expression—Total eye-specific RNA was extracted from 20 embryos (40 eyes) using the RNeasy micro kit (Qiagen) for both control (24, 27, 30, 36, and 48 hpf) and 1.5% ethanol-treated (27, 30, 36, and 48 hpf) embryos.

2.3.2 Whole embryo gene expression—Total RNA was extracted from snap frozen whole embryos (10 embryos each) using the RNeasy Mini kit (Qiagen) for untreated and treated embryos with or without thermal preconditioning.

The High Capacity cDNA Reverse Transcription kit with random primers (Applied Biosystems, Inc. [ABI], Foster City, CA) was used to synthesize the cDNA template for qRT-PCR. qRT-PCR was performed to determine the expression of genes (genes and primers are described in Supplemental Table 2) in untreated and ethanol-treated eyes of embryos. For each treatment and sampling time, three replicate measurements were performed, with β-actin as the endogenous reference gene. Primers were designed using primer express 3 (ABI, Foster City, CA; Supplemental Table 2). The 7900HT Fast Real-Time PCR System with SYBR-Green PCR Master Mix (ABI, Foster City, CA) was used for amplification. Mean Cycle threshold (Ct) from the three replicates was calculated prior to normalization [47].

2.4 Hsf-1 Immunocytochemistry

Cryosections were blocked with 20% goat serum in phosphate-buffered saline containing 0.5% Triton X-100 (PBST), and then were incubated with a rat monoclonal primary antibody (anti-human Hsf-1; Thermo-Scientific, Fremont, CA; # RT-405-P0) at 1:50 [48] overnight at 4°C. Sections were washed in PBST, and then were incubated with a goat anti-rat secondary antibody conjugated to Cy3 (Jackson Immunoresearch, West Grove, PA) at 1:200 for 2 hrs, were washed again and then mounted in Vectashield containing DAPI (Vector Laboratories, Burlingame, CA). Some sections were also processed for indirect immunofluorescence using the mouse monoclonal anti-HuC/D antibody (Life Technologies/Thermo Scientific, Grand Island, NY) at 1:200, detected with a donkey anti-mouse secondary antibody conjugated to FITC (Jackson Immunoresearch; 1:200). Sections were viewed using epifluorescence microscopy on a Leica DMR compound microscope, and were imaged with a SPOT digital camera and associated software. Images were combined using the “apply image” function in Adobe PhotoShopCS6 (Adobe Systems, San Jose, CA).

2.5 Western Blotting (Hsf-1)

To verify reactivity of the anti-human Hsf-1 antibody with zebrafish Hsf-1, a full-length cDNA encoding zebrafish Hsf-1 was cloned into the plasmid pEGFP-C1 (Clontech, Mountain View, CA) as in [49]. HeLa cells were transfected with pEGFP-C1-Hsf-1, or with pEGFP-C1, as previously [49]. Cells were incubated overnight, washed in PBS, and

collected in extraction buffer containing 1% nonidet P-40, 0.5% SDS, 50 mM Tris-HCl, and EDTA-free protease inhibitor cocktail (one tablet/7 mL; Roche Diagnostics, Indianapolis, IN) in PBS. These samples were centrifuged 13,000 rpm at 4°C for 20 min. Twelve μL of the supernatant was loaded per well and separated with a 10% polyacrylamide gel. Proteins were transferred to PVDF membranes, blocked with 5% bovine serum albumin in TBST, and immunoblotted with anti-Hsf-1 at 1:500 overnight. Chemiluminescent detection was carried out using a horseradish peroxidase-conjugated secondary antibody (2 hrs, 1:3000; Jackson Immunoresearch) and the Pierce ECL Western blotting substrate (Thermo Scientific).

2.6 Morpholino-Mediated Knockdown of hsf-1 mRNA

Antisense morpholino (MO) oligonucleotide injection was performed as described previously [50-53]. In brief, MOs were purchased from GeneTools LLC (Corvallis, OR), dissolved in a buffer (0.4 mM $MgSO_4$, 0.6 mM $CaCl_2$, 0.7 mM KCl, 58 mM NaCl, 25 mM HEPES pH 7.1), and heated to 65°C for 5 minutes prior to use. The MO targeting the start codon for *hsf-1* was described previously [40, 53]. The control MO was a non-specific control MO (with no complementary targets in zebrafish) described previously [54]. Approximately 3.0 nL of MO were injected into yolks of embryos at the one- or two-cell stage using methods previously described [50]. Our prior studies indicated that the minimal concentration of *hsf-1*-targeting MO that resulted in prevention of Hsf1 expression (as revealed by Western Blot) was 250 μM [53], and this concentration matches the concentration that, in a separate study [40], resulted in microphthalmia and cell death in the lens. This concentration (250 μM) was therefore considered “supra-threshold.” The sub-threshold concentration of *hsf-1*-targeting MO was 25 μM.

2.7 Thermal Preconditioning

Heat shock (thermal preconditioning) was applied to embryos in system water by incubating them for 1 hour at 37°C [55]. Following heat shock, embryos were exposed to 1.5% ethanol between 24 and 36 hpf at 28.5°C. Embryos were collected at 24 or 36 hpf and either were fixed with 4% paraformaldehyde for further tissue analysis or were snap frozen at -80°C using liquid nitrogen for RNA extraction.

2.8 Eye Measurements

Eye circumferences were measured as in [8, 13]. Paraformaldehyde-fixed embryos were placed on their sides in a petri dish. The left eyes of each embryo were photographed such that lens and eye boundaries were clearly visible. A Nikon stereomicroscope fitted with a CCD camera was used to image the eyes. The measurement tool in ImageJ/ScionImage software was used to measure eye circumference. Statistical analysis of eye measurements was done by using ANOVAs, followed by post hoc analyses (Fisher's test, with Bonferroni correction), as appropriate, and were performed using R statistical software [56]. A treatment was considered to result in significant microphthalmia if the average eye size of the treatment group was significantly smaller than that of the control group.

3. Results

3.1 Eye-Specific Gene Expression During Ethanol Exposure

To identify the genes that play critical roles in pathogenesis of ethanol-induced microphthalmia, we performed a time series microarray experiment using Affymetrix GeneChip Arrays on total RNA from dissected embryo eyes. The sampling times selected were based on the timing of known developmental processes that take place during retinal neurogenesis in the zebrafish embryo (Supplemental Table 1) [57], and based on prior

knowledge of the qualitative effects of ethanol exposure over this time [8]. The treatment initiation time roughly corresponds to day 14 of gestation in rodents; ethanol administration to pregnant rats at this time also results in microphthalmia [58]. Our experimental time course included an untreated control at 24 hpf prior to the exposure, 27 hpf samples (control and ethanol-treated) to detect early and acute effects of ethanol on retinal neurogenesis, and progressively distributed sampling times between 27 and 48 hpf (control and ethanol-treated). A single-replicate time series design was used specifically to extract information regarding developmental time-dependent effects of ethanol, while minimizing the sample quality risks incurred by the need to process, in parallel, large numbers of biological samples. This design is appropriate for statistical analysis with EDGE software, which as a spline function-based method, can detect significant temporal variation without a requirement for replicates at each sampling time of a time series [36, 38].

The raw microarray data were assessed for quality, subjected to normalization, and corrected for background. These raw data are available via the Gene Expression Omnibus (GEO; accession #GSE51427). To compare gene expression in treated vs. untreated samples, we analyzed the data represented as RMA expression using two different algorithms. These analyses were used to select genes for validation of microarray results and for identifying biological processes of interest for functional studies of their involvement in mediating ethanol toxicity to the eye.

3.1.1 SAM analysis—This approach was used to identify differentially expressed genes in ethanol-treated as compared to control eyes. A scatter plot of the observed relative difference d(i) vs the expected relative difference $d_E(i)$ is provided as Figure 1A. For the majority of the genes $d(i) \approx d_E(i)$, but some genes are represented by points displaced from the $d(i) = d_E(i)$ line by a distance greater than a threshold $\Delta = 2$ (dotted lines). This approach yielded 62 significantly differentially expressed genes in the ethanol treated eyes (green circles in Fig. 1A) at a false discovery rate of 0.102 (predicted number of falsely called genes = 9.5). Supplemental Tables 3 and 4 show detailed lists of up-regulated and down-regulated genes, respectively, along with corresponding SAM scores or test statistics (d-values) and fold changes.

3.1.2 EDGE algorithm—We performed a 'between class' EDGE analysis [44] to identify differences in expression over time in ethanol-treated embryo eyes as compared to untreated embryo eyes. For this analysis, RMA expression was normalized and no data filters were used. In ***Approach 1*** of this analysis, a time course analysis was run using EDGE with all arrays (all control and ethanol-treated, unbalanced). This approach identified 2039 genes with a q-value (significance value or threshold) cut-off of 0.05 [59]. The top 95 genes differentially expressed in treated eyes, ranked by p-value, are listed in Supplemental Table 5. In ***Approach 2***, a time course analysis was run with treated and control groups using the EDGE algorithm, but with artificial replication of the 24 hpf control sample in order to balance the analysis (equal number of control and ethanol-treated samples). This approach identified 3865 genes with a q-value cut-off of 0.05. 1593 genes of the 2039 differentially expressed genes from Approach 1 were identified as differentially expressed in Approach 2 (Fig. 1B).

Lists of differentially expressed genes obtained from all three approaches (SAM, and the two EDGE approaches) have common genes (Fig. 1B). The number of genes common to all lists, however, was quite low (5 genes). This is not surprising given that the EDGE algorithm is fundamentally quite different from SAM as it takes into account the temporal changes in gene expression, while SAM as applied in this study is blind to developmental time. We performed a gene ontology (GO) analysis of the differentially expressed gene sets from the EDGE2 approach using a web based tool, GOEAST [45]. Several biological

processes, including cholesterol metabolic process, cellular homeostasis, central nervous system development, and response to stress (Fig. 1C; Supplemental Table 6) were represented in the differentially expressed lists, according to the GO analysis. More specifically, several key components of the cellular stress (i.e. “heat shock”) response were either significantly up-regulated (*hsp-40* homolog) or down-regulated (*hsf-1*) in eyes following embryonic ethanol exposure (Fig. 1B, Supplemental Tables 3, 4, 5).

Using the set of 2039 differentially expressed genes identified by EDGE1 analysis (Fig. 1B), an average-linkage, hierarchical clustering was performed in R, on mean-centered data (centered by differentially expressed genes, as in [46]), and the output is shown as a heatmap in Supplemental Figure 1. The two major categories of differentially expressed genes – those that are predominantly downregulated over developmental time vs. those that are predominantly upregulated over developmental time - showed only minor differences (ethanol vs. control) from 24 to 36 hpf. However, large differences in the patterns of expression of differentially expressed genes became evident at 48 hpf (Supplemental Fig. 1).

We next used a complementary approach to evaluate expression of selected genes during ethanol exposure, by mining our microarray dataset. We specifically examined the RA and Shh cellular signaling systems implicated in the pathogenesis of FASD, as well as additional genes associated with eye development, cell cycle progression, and the cellular stress response. In our microarray analysis, the RA signaling related genes *rxrβa*, *rxrαb*, and *nr2f5* were differentially regulated over time in ethanol-treated as compared to control eyes, according to EDGE analysis (Fig. 2A). However, the majority of genes related to RA signaling were not differentially regulated according to any of the analyses, including those encoding the RA synthesizing enzyme Aldh1a2 and the RA catabolic enzyme Cyp26 (Supplemental Table 7). These findings are in general agreement with our previous study [13] demonstrating that RA signaling is not involved in causing ethanol-induced microphthalmia over the period of retinal neurogenesis. However, the microarray results suggest that ethanol does have some effects on temporal expression patterns of a subset of RA-related genes within the eye.

The Shh signaling system is also implicated as mediating effects of ethanol exposure on embryonic development [12, 24, 25]. In our microarray analysis, the Shh signaling related genes *shha*, *hhip*, *gli3*, *smo*, *gli2b*, and *sufu* were differentially regulated over time in ethanol-treated as compared to control eyes, according to EDGE analyses (Fig. 2A), suggesting potential effects of ethanol exposure on temporal patterns of expression of Shh signaling components. However, the majority of genes related to Shh signaling were not differentially regulated according to any of the analyses, including the Shh signaling targets *ptch1* and *ptch2* (Supplemental Table 7), and those that were differentially regulated were predominantly increased in expression (Fig. 2A). These findings are also in general agreement with our prior study indicating that Shh signaling within the eye is not involved in causing ethanol-induced microphthalmia over the period of retinal neurogenesis [13].

Several genes related to the regulation of the cell cycle were also further evaluated. EDGE analyses indicated that several *cyclin* genes (*ccng2*, *ccna1*, *ccng1*, and *ccnd1*), along with *pcna* and *mcm5*, showed significantly different temporal expression patterns in ethanol-treated as compared to control eyes (Fig. 2B). Most cyclins (*ccng2*, *ccna1*, *ccng1*, *ccnd1*) showed an increase in expression in ethanol-treated as compared to control eyes, while the cyclin-dependent kinase *cdk2* was decreased in expression (Fig. 2B). These results are consistent with the recent study by Chung et al. [14] indicating that embryonic ethanol exposure results in sustained cyclin expression and possibly failure of retinal neurons to exit the cell cycle and differentiate [8, 14].

During retinal neurogenesis, ethanol causes reduced cell differentiation, particularly that of photoreceptors [8, 14]. However, this effect is not likely due to changes in expression of genes involved in initiation of retinal neurogenesis (*ath5/atoh7*, *pax6*) or in photoreceptor determination genes (*crx*, *rx-1*, *neuroD*)[8, 14]. These results were confirmed in our time series microarray, in which no significant changes were observed in RMA expression of these genes following ethanol treatment as compared to control (data not shown). However, other genes related to eye development were significantly differentially expressed in ethanol-treated eyes (Fig. 2C). These include the photoreceptor genes *rhodopsin* and *interphotoreceptor binding protein* (*irbp*) [60, 61], and genes encoding the developmental signaling factors *wnt11* [62] and *gdf6a* [63].

The lists of differentially expressed genes included numerous genes related to the cellular stress response (Fig. 1B,C; Supplemental Tables 3, 4, 5), prompting us to investigate the nature of this differential expression as a function of time during treatment. Figure 2D shows heatmaps representing % change in RMA expression of selected, differentially-expressed stress response genes, in control as compared to ethanol-treated eyes. For the majority of the cellular stress response genes, this difference appeared to be a reduction in expression as compared to controls (*hsf1, hsf2, hsbp1, dnaja2, dnajb6a, dnajb11, dnajc11*), or an up-regulation only at the last sampling time (*hsp-70*). This was unexpected because these components of the cellular stress response are normally rapidly up-regulated in response to environmental stressors, including a variety of toxins [64].

3.2 Validation of Microarray by qRT-PCR

Additional genes were selected from the EDGE and SAM analyses for validation of microarray using qRT-PCR. H2A histone family, member X (*h2afx*; GeneID:394048) encodes a histone variant involved in transcriptional regulation and DNA repair [65], and *cyclin G1*(GeneID; 2437408 [66]) encodes an important factor in the control of cell cycle, through its regulating activity of cyclin-dependent kinases [67]. Expression levels of each were evaluated and validated using qRT-PCR, and in each case changes in expression corresponded to those measured with microarray (Supplemental Fig. 2) in both treated and untreated embryos. We have previously reported expression levels of *ptch2* (*ptc2*), *shha*, and *nr2f5* at 24, 27, 30, 36, and 48 hpf, as measured by qRT-PCR of eye tissues of ethanol-treated and untreated embryos [13]. The temporal patterns of expression of these genes corresponded to those measured in the present study with microarray analysis, providing additional validation of the microarray results.

3.3 Heat Shock Response: hsf-1 and hsp-70

In this study, several components of the cellular stress response were differentially expressed, but paradoxically down-regulated, or with a large temporal delay before up-regulation (Fig. 1B; 2D; Supplemental Tables 3, 4, 6). Of great interest to this study, Lele and colleagues [68] observed induction of *hsp-70* at low levels with an acute, high dose ethanol exposure (4% for 4 hours). In the present study, a more chronic (24 hour) and lower dose (1.5%) exposure resulted in delayed *hsp-70* mRNA up-regulation in treated groups (Fig. 1B; 2D; Fig. 3A). Consistent with the microarray, significant up-regulation of *hsp-70*, measured by qRT-PCR, was detected only at the last sampling time, 48 hpf (Fig. 3B), 24 hours later than the initial ethanol exposure. It is known that heat shock as a stressor causes up-regulation of *hsp-70*, with maximal expression around 8 hours [68]. In ethanol-treated embryos, this delay in the cellular stress response may therefore be related to the pathological outcome of microphthalmia.

The cellular response to heat shock includes two sets of important players, Hsfs and Hsps. Hsfs are transcription factors that bind to heat shock elements (HSEs) on the promoters of

the heat shock genes and activate their transcription. In the present study, ethanol treatment of embryonic zebrafish eyes resulted in reduction of *hsf-1* as identified by SAM analysis of microarray, and by both EDGE analyses (Fig. 1B; Supplemental Table 4; Fig. 2D). It was very surprising that *hsf-1* was down-regulated (fold change small, but highly statistically significant, p=0.0002; Fig. 3C), as Hsf-1 expression is known to be induced by stress and environmental toxins [64]. As the expression levels of *hsf-1* in embryonic zebrafish eyes were extremely low (Fig. 3C), we were not able to reliably detect *hsf-1* using *in-situ* hybridization, nor were we able to reliably detect low fold changes in eye tissues using qRT-PCR (although the primers amplified *hsf-1* sequence from whole embryos and adult retina; data not shown).

3.4 Hsf-1 Protein Distribution in Ethanol-Treated Embryos

In order to characterize any changes in Hsf-1 protein within the embryonic eye as a consequence of ethanol exposure, we performed indirect immunofluorescence experiments using an anti-Hsf-1 antibody [69]. In untreated embryos fixed at 36 hpf, Hsf-1 protein was present in a subpopulation of cells within the developing brain, consistent with the *hsf-1 in situ* hybridization results of [70], and appeared to colocalize with DAPI, suggesting a nuclear localization (Fig. 4A, B). Hsf-1 protein was also present within the embryonic retina, primarily though not exclusively within a population of cells at the future vitreal surface; these may correspond to developing retinal ganglion cells, and in some cases these cells co-expressed the neuronal marker HuC/D (Fig. 4C). In two of 12 embryos analyzed, we also observed Hsf-1immunoreactivity in nuclei of lens epithelial cells (data not shown). In embryos treated with 1.5% ethanol at 24 hpf and processed at 36 hpf, Hsf-1-positive cells within the retina were not observed, and very few Hsf-1-positive cells were present in the brain (Fig. 4D-F; images are representative of 3 separate experiments, 3-6 embryos evaluated from each experiment). These results suggest that a consequence of embryonic ethanol exposure during retinal neurogenesis is a down-regulation of Hsf-1 protein within cells of the developing eye.

To establish the rate at which a reduction in *hsf-1* mRNA may result in changes in Hsf-1 protein within the eye, we performed additional immunofluorescence experiments on samples obtained at 27 and 30 hpf. At 27 hpf, ethanol-treated embryos (n=8) showed a distribution of Hsf-1 immunoreactivity similar to that seen in controls (n=7) (Supplemental Fig. 3A,B), while at 30 hpf, ethanol-treated embryos (n=10) showed several patterns of Hsf-1 immunoreactivity as compared to controls (n=9) (Supplemental Fig. 3C-F). Three ethanol-treated embryos showed no Hsf-1-positive cells in the retina, five showed reduced staining in the retina, and two showed strong staining in the retina, similar to controls. These data suggest that the reduced *hsf-1* mRNA detected by the microarray led to reduced Hsf-1 protein in the retina by 30 hpf or soon thereafter.

3.5 Verification of Hsf-1 Antibody

Reactivity of the Hsf-1 antibody with zebrafish Hsf-1 protein was verified by Western blot, using HeLa cells transfected with a plasmid encoding a zebrafish Hsf-1-EGFP (enhanced green fluorescent protein) fusion protein, or with a plasmid containing the coding sequence for EGFP. Figure 5A shows a representative Western blot of protein obtained from EGFP-transfected HeLa cells (first lane), and protein obtained from cells transfected with the zebrafish Hsf-1-EGFP plasmid (remaining three lanes). In all four lanes, a band is detected that is the predicted molecular weight of human HSF-1 (huHSF-1; approximately 85 kDa). In the final three lanes, an additional band is detected that is the predicted molecular weight of the fusion protein (zfHsf-1-EGFP; approximately 150 kDa) (see also [49]), indicating that the anti-human Hsf-1 antibody used in these studies also detects the zebrafish Hsf-1 protein.

As an additional test of the Hsf-1 antibody in zebrafish tissues, we performed indirect immunofluorescence experiments on sections derived from embryos treated with supra-threshold levels of a validated *hsf-1* MO [40, 49] at the one- to two-cell stage, and fixed at 48 hpf. In sections derived from untreated embryos, Hsf-1 immunoreactivity was found in the retina, in the emerging ganglion cell layer and inner nuclear layer, and with a nuclear localization (Fig. 5B-C). A similar labeling pattern was observed in sections derived from embryos treated with a control MO (Fig. 5D-E). This labeling pattern was not evident in sections derived from *hsf-1* morphants (Fig. 5F-G), providing evidence that the Hsf-1 antibody used in these studies [48] detects Hsf-1 protein in zebrafish tissues.

3.6 Ethanol and Hsf-1 Pathway Interaction Studies

We next performed studies to test whether ethanol and reduced levels of Hsf-1 functioned via a similar molecular pathway in the generation of microphthalmic phenotypes. We combined sub-threshold levels of *hsf-1* MO (those that do not result in an eye phenotype; [53] (Fig. 6E) with sub-threshold levels of ethanol (0.5%, which does not result in significant microphthalmia [8]; Fig. 6B). One- to two-cell stage embryos were injected with sub-threshold or supra-threshold levels of a previously validated *hsf-1* MO [40, 53], or with a control MO that does not target any zebrafish nucleic acid sequence [54], and then these embryos were treated with 0.5% or 1.5% ethanol at 24 hpf and were examined at 36 hpf or 48 hpf. In these experiments, embryos treated with 1.5% ethanol (Fig. 6C), or those treated with a combination of sub-threshold *hsf-1* MO and sub-threshold ethanol (Fig. 6F) showed significant microphthalmia at 36 hpf, and at 48 hpf (Fig. 6G, I; $p<0.05$ compared to untreated controls; ANOVA followed by post-hoc analysis). The same experimental conditions also resulted in significantly reduced lens size (Fig. 6H; $p<0.05$ compared to untreated controls; ANOVA followed by post-hoc analysis). Embryos treated with a combination of control MO and 0.5% ethanol showed eye sizes similar to those of untreated controls (Fig. 6I). We were also able to verify that supra-threshold concentrations of *hsf-1* MO resulted in significant microphthalmia at 48 hpf (Fig. 6I; $p<0.05$ compared to untreated controls; ANOVA followed by post-hoc analysis; see also Fig. 5F-G).

3.7 Rescue Studies: Thermal Preconditioning

The microphthalmic effects of *hsf-1* knockdown [40], the reduced Hsf-1 expression in eyes of ethanol-treated embryos (Fig. 4; Supplemental Table 4; Fig. 2D), and the evidence supporting common molecular pathways for the effects of ethanol and *hsf-1* knockdown (Fig. 6), together prompted us to test if ethanol-induced microphthalmia could be rescued by manipulation of the cellular stress response. We initially attempted overexpression of *hsf-1* capped mRNA, but this strategy did not result in accumulation of Hsf-1 protein in eyes of treated embryos, nor did it result in rescue of eye size in ethanol-treated embryos (data not shown). It is possible that *hsf-1*mRNA experiences rapid turnover and may lack the perdurance *in vivo* to initiate a response sufficient for rescue [71].

As an alternative, we next used thermal preconditioning, which activates Hsf-1 [72], and correspondingly up-regulates expression of *hsp-70* mRNA [53, 73, 74]. We predicted that this activation process, prior to ethanol exposure, may stimulate necessary chaperone expression and functions to counteract the effects of ethanol. Thermal preconditioning (mild heat shock; HS) is a method commonly employed in studies of ischemia such that a mild preconditioning reduces damage related to ischemia or hypoxia [75]. We designed two different experimental approaches for using thermal preconditioning to test for rescue effects. 1) HS (37°C, 1 hour) was applied at 16 hpf, 8 hours prior to ethanol exposure; 2) HS (37°C, 1 hour) was applied at 14 hpf, 10 hours prior to ethanol exposure. The HS at 16 hpf (Fig. 7A), resulted in a partial prevention of ethanol-induced microphthalmia; the eye circumferences of the ethanol-treated HS embryos were not significantly different from

those of the HS embryos, but remained significantly different from untreated controls (ANOVA, followed by post hoc analysis; $p < 0.05$). Surprisingly, HS at 14 hpf was not effective at rescuing microphthalmia (Fig. 8B).

To evaluate our thermal preconditioning rescue strategy, we measured *hsp-70* mRNA expression following each of the thermal preconditioning approaches. We observed significant up-regulation *of hsp-70* expression at 24 hpf following HS at 16 hpf (8 hours after HS; Fig. 7C), coinciding with the time of experimental exposure to ethanol. These results are consistent with the observation of partial prevention of the small eye phenotype with 16 hpf HS protocol. These results suggest that thermal preconditioning, and consequent up-regulation *of hsp-70*, has a modest protective effect for preventing ethanol-induced microphthalmia. Interestingly, *hsp-70* up-regulation at 24 hpf was not observed with the 14 hpf HS approach (10 hours after HS; Fig. 7C). This outcome provides support to the idea that thermal preconditioning partially prevents ethanol-induced microphthalmia only when high *hsp-70* levels are generated at the time of ethanol exposure. The lack of significant *hsp-70* induction 10 hours after the 14 hpf heat shock was itself surprising, and suggests that the cellular stress response (to thermal preconditioning) is complex and dynamic during embryonic development.

To test whether the expression or distribution of Hsf-1 was altered by thermal preconditioning, embryos obtained from a 16 hpf HS experiment were processed for indirect immunofluorescence with the Hsf-1 antibody. Control (no HS, no ethanol) embryos displayed Hsf-1-positive nuclei in brain and retina (Fig. 8A, B), and ethanol-treated embryos lacked Hsf-1-positive nuclei in retina (Fig. 8E, F). Embryos subjected to HS at 16 hpf showed a similar distribution of Hsf-1-positive nuclei in retina, intense staining of nuclei in brain, and in six of seven embryos analyzed, nuclei of lens epithelial cells were also stained (Fig. 8C, D). Of greatest interest, we observed Hsf-1-positive nuclei in retinas and lenses of eight embryos that were subjected to HS at 16 hpf and then treated with ethanol at 24 hpf (Fig. 8G, H). These findings, together with those related to *hsp-70* expression (Fig. 8C) suggest that the 16 hpf thermal preconditioning protocol was successful at engaging the heat shock response by the time of ethanol treatment, such that a partial prevention of the microphthalmic effects of ethanol was achieved.

4. Discussion

Ethanol treatment of zebrafish embryos during retinal neurogenesis results in microphthalmia associated with retina and lens abnormalities [8]. The objective of this study was to identify genes and biological processes that are altered by ethanol in the eyes of embryonic zebrafish by using time series microarray. In this study, we assayed zebrafish embryo eyes (control and ethanol-treated) at different sampling times (24, 27, 30, 36, and 48 hpf) during retinal neurogenesis. A striking observation in our study was the existence of changes in expression of numerous genes involved in the cellular stress (“heat shock”) response. We tested the hypothesis that the heat shock response is involved in the microphthalmic response of zebrafish embryo eyes to ethanol by performing combined treatment with sub-threshold levels of ethanol and morpholino targeting *hsf-1*. This combined treatment resulted in microphthalmia, suggesting a common molecular pathway for ethanol and *hsf-1* knockdown. In addition, we were able to achieve a partial rescue of microphthalmia by using thermal preconditioning to sustain Hsf-1 protein, and up-regulate a key player in heat shock response, *hsp-70*. Together these results suggest a role for the heat shock response in mediating the ocular effects of ethanol in embryonic zebrafish.

4.1 Time Series Microarray Analysis

We report for the first time an application of time series microarray to study the changes in gene expression induced by ethanol during development. The molecular mechanisms underlying ethanol toxicity in embryos are largely unknown in zebrafish, particularly with respect to ethanol exposures during the time of retinal neurogenesis [8, 13]. Our time series microarray analysis is an important step toward identifying these mechanisms.

The multiple analysis approach (SAM and EDGE) together with GO analysis of microarray revealed several genes common to two or more of the analyses. These genes belonged to distinct but interrelated molecular pathways. Many of these genes were related to the heat shock response, cell cycle regulation, developmental processes, and response to stimulus. Similar changes in gene profiles were previously detected in microarray of whole brain of ethanol-treated vs. control embryonic mouse, including changes in genes related to cell cycle regulation and differentiation [30].

We mined the present microarray dataset to evaluate the most commonly implicated signaling systems in developmental toxicity of ethanol: retinoic acid signaling, and Sonic hedgehog signaling. RA signaling is known to play a key role in development of ethanol targets, including the central nervous system, heart, limbs and eyes [76]. Ethanol may reduce RA signaling by competitively inhibiting the dehydrogenase enzymes involved in RA synthesis [20, 77, 78]. Several studies have provided evidence of reduced levels of RA due to ethanol exposure and/or demonstrated that administration of RA could rescue the phenotypes caused by ethanol in animal models [21, 22, 79, 80]. In contrast, the microphthalmic effects of ethanol treatment during retinal neurogenesis were not rescued with addition of RA [13]. Consistent with these prior results, the present microarray study revealed no significant changes in expression of numerous RA signaling-related genes within the eye, including retinoid binding proteins, retinoid receptors, and retinoid metabolizing enzymes (Supplemental Table 7). However, three RA signaling-related genes were significantly differentially expressed over time in ethanol-exposed eyes: the receptors *RXRβa* and *RXRαb*, and the orphan nuclear receptor *nr2f5* (Fig. 2A), which is known to act as a negative regulator of RA. These results suggest some effects of ethanol on the temporal expression dynamics of a small subset of RA-related genes during retinal neurogenesis.

We also evaluated the Shh signaling system, which is frequently indicated as a potential mediator of developmental effects of ethanol exposure. Ethanol treatment during gastrulation and neurulation results in axial defects and craniofacial defects including microphthalmia, that can be rescued by administration of Shh [25], or by injection of supplemental cholesterol [24], a component of the mature Shh lipoprotein [81]. The present study identified several Shh signaling-related genes as differentially expressed over time in ethanol-exposed eyes, including *shha* (Fig. 2A). Interestingly, all of these genes showed increases in expression over time as compared to control eyes. These findings, along with the large number of additional Shh signaling-related genes that were not differentially expressed (Supplemental Table 7), are consistent with our prior study demonstrating that reduced Shh signaling within the eye does not underlie the microphthalmic phenotype generated by ethanol exposure during retinal neurogenesis [13]. These findings do not discount previous studies indicating that ethanol affects Shh expression and/or signaling at earlier developmental times and in non-ocular tissues [21, 23, 24].

Several genes related to cell cycle progression were also detected by the microarray analysis as differentially expressed over time in eyes exposed to ethanol during retinal neurogenesis. The increased expression of several cyclins (as compared to control) and decreased expression of *cdk2* together suggest that cells of the eye may fail to exit the cell cycle. Interestingly, zebrafish embryos treated continuously with 1.5% ethanol over the first 48 hrs

of development also show disruptions in expression of genes related to cell cycle progression and withdrawal [14].

A detailed inspection of the genes with altered expression indicated striking changes in many mRNAs coding for components of the heat shock pathway. Similar to our observation of altered *hsp* and *hsf* genes in ethanol-treated embryo eyes, a number of other microarray studies of ethanol effects in adult cortex of humans and mouse suggest that ethanol treatment alters expression of some of the *hsp* genes [82-85] [82, 83, 85, 86], which in turn may be important in the pathophysiological responses to ethanol. The next Section (4.2) will introduce a model in which the ocular effects of ethanol may be mediated by changes in expression of components of the heat shock response.

4.2 Embryonic Ethanol Exposure and the Heat Shock Response

The microarray results, along with Hsf-1 immunocytochemistry and *hsp-70* qRT-PCR, suggested the involvement of several components of the cellular stress response in eyes of ethanol-treated embryos. Previous studies of these components of the heat shock response revealed requirements for both *hsf-1* and *hsp-70* in the support of lens and eye development, with significant microphthalmia resulting from morpholino-mediated knockdown of either component [40, 87]. To test the hypothesis that the microphthalmic effects of ethanol exposure during retinal neurogenesis are mediated by reduced expression of *hsf-1*, we treated embryos with sub-threshold *hsf-1* MO, together with sub-threshold (0.5%) ethanol. These embryos displayed significant microphthalmia (Fig. 7), consistent with reduced *hsf-1* and ethanol treatment acting by a common molecular pathway. In further support of this hypothesis, a thermal preconditioning protocol that elevated *hsp-70* mRNA expression at the time of ethanol administration (24 hpf; Fig. 8) and sustained Hsf-1 protein expression in the presence of ethanol (Fig. 9), was successful in partially preventing microphthalmia (Fig. 8).

We propose a working model to describe the role of the heat shock response in ethanol induced microphthalmia, and to suggest how manipulation of this system may partially prevent the effects of ethanol. Hsf-1 activation (translocation into the nucleus) is known to be initiated by either a stress stimulus or a developmental process and is mediated by phosphorylation of serine residues of Hsf-1 [88]. This results in binding of Hsf-1 to HSEs, and activation of transcription of *hsp* mRNAs such as *hsp-70* [39]. The *hsp* genes encode molecular chaperones that facilitate protein folding and prevent aggregation of mis-folded proteins, thereby supporting cell survival and proper cell function [89]. In mouse, Hsf-4 has been shown to have additional regulatory targets, including genes encoding fibroblast growth factors, which in turn influence development of the ocular lens [90].

We suggest that ethanol also acts on the heat shock response system, but paradoxically down-regulates *hsf-1* mRNA, resulting in reduced Hsf-1 within the developing eye (within approximately 6 hours), and delayed up-regulation of *hsp-70* in response to the ethanol stress. During the resultant period of insufficient Hsp-70 for responding to the effects of ethanol stress, a cascade of events occurs, culminating in microphthalmia. It is tempting to speculate that this cascade of events includes cell death in the lens following ethanol exposure [8], resulting in abnormal lens development and microphthalmia. In support of this idea, roles for *hsf-1* and *hsp-70* in promoting lens survival and consequently, eye growth, have been demonstrated [40, 87, 91]. However, we only reliably detected Hsf-1 protein within the lenses of embryos that were subjected to thermal preconditioning, suggesting that unstressed, developing embryos may not activate Hsf-1 within lens tissues to an extent that is readily detectable by immunocytochemistry. Consistent with this working model, several *hsp40* genes (*dnajb6a*, *dnajb11*, *dnajc11*) were also significantly differentially expressed (reduced in expression) following embryonic ethanol exposure in our time-series microarray (Fig. 1B; Supplemental Tables 3-6). Furthermore, we note that EDGE analysis identified

hypoxia inducible factor 1a (*hif-1a*) as significantly differentially expressed over time in eyes of ethanol-treated embryos, with upregulation taking place at 48 hpf (Supplemental Table 5; data not shown). Since Hif-1a can interact with the *hsp-70* promoter [49, 92], it is possible that Hif-1a activity was responsible for the upregulation *of hsp-70* at the end of the ethanol treatment period.

Our strategy for manipulation of the cellular stress response was the use of thermal preconditioning. Preconditioning with mild heat shock has been shown to protect cells from severe stressors [75, 93, 94]. We predicted that up-regulation of this response as a consequence of thermal preconditioning would result in molecular activities that would counteract the effects of ethanol exposure. The activated cellular response prepares developing tissues for additional stress (in the present study, in the form of ethanol), thereby preventing cell death or abnormal cell function [93]. The outcome in the present study was near-normal development of the eye. Studies in heart and brain in animal models have demonstrated the potential of using thermal preconditioning as a therapeutic agent in reducing damage by ischemic injury [49, 75, 94-96], and Hsf-1 specifically has been considered a pharmacological target for Huntington's Disease [97]. Our studies suggest that the Hsf-1 and Hsp-70 may also be considered reasonable therapeutic targets for fetal alcohol exposure. We note that any intervention targeting these components of the cellular stress response would be most likely administered to women who know they are pregnant, but continue to drink, a situation that is associated with other circumstances such as abuse or prenatal health problems [98]. In this scenario an intervention treatment would potentially counteract the effects of ethanol during the period of organogenesis, a developmental time that corresponds to the time frame of our experimental protocols in zebrafish.

Supplementary Material

Refer to Web version on PubMed Central for supplementary material.

Acknowledgments

The authors thank Mr. Sam Hunter (U. Idaho) for assistance with microarray design and analysis. Microarray procedures were performed at the Genomics Core of the UI/WSU Center for Reproductive Biology, Washington State University (Pullman, WA). Funding for this work was provided by NIH R01 EY012146 (DLS), NSF IOS-0818993 (EAS), pilot project funding from P20 RR016454 (Idaho INBRE) and P20 RR015587 (COBRE) (DLS), University of Idaho's BANTech (Biological Applications of Nanotechnology) program (DLS), a University of Idaho Student Grant Program award to BK, and a Department of Biological Sciences undergraduate research award to LP.

References

1. Riley EP, Infante MA, Warren KR. Fetal alcohol spectrum disorders: an overview. Neuropsychology review. 2011; 21:73–80. [PubMed: 21499711]
2. Vernescu RM, Adams RJ, Courage ML. Children with fetal alcohol spectrum disorder show an amblyopia-like pattern of vision deficit. Developmental medicine and child neurology. 2012; 54:557–62. [PubMed: 22574626]
3. Stromland K, Pinazo-Duran MD. Ophthalmic involvement in the fetal alcohol syndrome:clinical and animal model studies. Alcohol Alcohol. 2002; 37:2–8. [PubMed: 11825849]
4. Aoto K, Shikata Y, Higashiyama D, Shiota K, Motoyama J. Fetal ethanol exposure activates protein kinase A and impairs Shh expression in prechordal mesendoderm cells in the pathogenesis of holoprosencephaly. Birth Defects Res A Clin Mol Teratol. 2008; 82:224–31. [PubMed: 18338389]
5. Green ML, Singh AV, Zhang Y, Nemeth KA, Sulik KK, Knudsen TB. Reprogramming of genetic networks during initiation of the Fetal Alcohol Syndrome. Dev Dyn. 2007; 236:613–31. [PubMed: 17200951]

6. Blader P, Strahle U. Ethanol impairs migration of the prechordal plate in the zebrafish embryo. Dev Biol. 1998; 201:185–201. [PubMed: 9740658]
7. Loucks EJ, Schwend T, Ahlgren SC. Molecular changes associated with teratogen-induced cyclopia. Birth Defects Res A Clin Mol Teratol. 2007; 79:642–51. [PubMed: 17647295]
8. Kashyap B, Frederickson LC, Stenkamp DL. Mechanisms for persistent microphthalmia following ethanol exposure during retinal neurogenesis in zebrafish embryos. Vis Neurosci. 2007; 24:409–21. [PubMed: 17640445]
9. Bilotta J, Saszik S, Givin CM, Hardesty HR, Sutherland SE. Effects of embryonic exposure to ethanol on zebrafish visual function. Neurotoxicol Teratol. 2002; 24:759–66. [PubMed: 12460658]
10. Matsui JI, Egana AL, Sponholtz TR, Adolph AR, Dowling JE. Effects of ethanol on photoreceptors and visual function in developing zebrafish. Invest Ophthalmol Vis Sci. 2006; 47:4589–97. [PubMed: 17003456]
11. Dlugos CA, Rabin RA. Ocular deficits associated with alcohol exposure during zebrafish development. J Comp Neurol. 2007; 502:497–506. [PubMed: 17394139]
12. Zhang C, Turton QM, Mackinnon S, Sulik KK, Cole GJ. Agrin function associated with ocular development is a target of ethanol exposure in embryonic zebrafish. Birth Defects Res A Clin Mol Teratol. 91:129–41. [PubMed: 21308976]
13. Kashyap B, Frey RA, Stenkamp DL. Ethanol-induced microphthalmia is not mediated by changes in retinoic acid or sonic hedgehog signaling during retinal neurogenesis. Alcohol Clin Exp Res. 2011; 35:1644–61. [PubMed: 21554333]
14. Chung HY, Chang CT, Young HW, Hu SP, Tzou WS, Hu CH. Ethanol inhibits retinal and CNS differentiation due to failure of cell cycle exit via an apoptosis-independent pathway. Neurotoxicol Teratol. 2013; 38:92–103. [PubMed: 23714372]
15. Loucks EJ, Ahlgren SC. Deciphering the role of Shh signaling in axial defects produced by ethanol exposure. Birth Defects Res A Clin Mol Teratol. 2009
16. Marrs JA, Clendenon SG, Ratcliffe DR, Fielding SM, Liu Q, Bosron WF. Zebrafish fetal alcohol syndrome model: effects of ethanol are rescued by retinoic acid supplement. Alcohol (Fayetteville, NY). 44:707–15.
17. Bilotta J, Barnett JA, Hancock L, Saszik S. Ethanol exposure alters zebrafish development: a novel model of fetal alcohol syndrome. Neurotoxicol Teratol. 2004; 26:737–43. [PubMed: 15451038]
18. Buske C, Gerlai R. Early embryonic ethanol exposure impairs shoaling and the dopaminergic and serotoninergic systems in adult zebrafish. Neurotoxicol Teratol. 33:698–707. [PubMed: 21658445]
19. Loucks E, Carvan MJ 3rd. Strain-dependent effects of developmental ethanol exposure in zebrafish. Neurotoxicol Teratol. 2004; 26:745–55. [PubMed: 15451039]
20. Deltour L, Ang HL, Duester G. Ethanol inhibition of retinoic acid synthesis as a potential mechanism for fetal alcohol syndrome. Faseb J. 1996; 10:1050–7. [PubMed: 8801166]
21. Marrs JA, Clendenon SG, Ratcliffe DR, Fielding SM, Liu Q, Bosron WF. Zebrafish fetal alcohol syndrome model: effects of ethanol are rescued by retinoic acid supplement. Alcohol (Fayetteville, NY). 2009
22. Yelin R, Schyr RB, Kot H, Zins S, Frumkin A, Pillemer G, et al. Ethanol exposure affects gene expression in the embryonic organizer and reduces retinoic acid levels. Dev Biol. 2005; 279:193–204. [PubMed: 15708568]
23. Brennan D, Giles S. Sonic hedgehog expression is disrupted following in ovo ethanol exposure during early chick eye development. Reproductive toxicology. 2013
24. Li YX, Yang HT, Zdanowicz M, Sicklick JK, Qi Y, Camp TJ, et al. Fetal alcohol exposure impairs Hedgehog cholesterol modification and signaling. Lab Invest. 2007; 87:231–40. [PubMed: 17237799]
25. Ahlgren SC, Thakur V, Bronner-Fraser M. Sonic hedgehog rescues cranial neural crest from cell death induced by ethanol exposure. Proc Natl Acad Sci U S A. 2002; 99:10476–81. [PubMed: 12140368]
26. Porter JA, Young KE, Beachy PA. Cholesterol modification of hedgehog signaling proteins in animal development. Science. 1996; 274:255–9. [PubMed: 8824192]

27. Concordet JP, Lewis KE, Moore JW, Goodrich LV, Johnson RL, Scott MP, et al. Spatial regulation of a zebrafish patched homologue reflects the roles of sonic hedgehog and protein kinase A in neural tube and somite patterning. Development. 1996; 122:2835–46. [PubMed: 8787757]
28. Downing C, Flink S, Florez-McClure ML, Johnson TE, Tabakoff B, Kechris KJ. Gene expression changes in C57BL/6J and DBA/2J mice following prenatal alcohol exposure. Alcohol Clin Exp Res. 36:1519–29. [PubMed: 22530671]
29. Da Lee R, Rhee GS, An SM, Kim SS, Kwack SJ, Seok JH, et al. Differential gene profiles in developing embryo and fetus after in utero exposure to ethanol. Journal of toxicology and environmental health. 2004; 67:2073–84. [PubMed: 15513904]
30. Hard ML, Abdolell M, Robinson BH, Koren G. Gene-expression analysis after alcohol exposure in the developing mouse. The Journal of laboratory and clinical medicine. 2005; 145:47–54. [PubMed: 15668661]
31. Wang LL, Zhang Z, Li Q, Yang R, Pei X, Xu Y, et al. Ethanol exposure induces differential microRNA and target gene expression and teratogenic effects which can be suppressed by folic acid supplementation. Human reproduction (Oxford, England). 2009; 24:562–79.
32. Zhou FC, Zhao Q, Liu Y, Goodlett CR, Liang T, McClintick JN, et al. Alteration of gene expression by alcohol exposure at early neurulation. BMC Genomics. 2011; 12:124. [PubMed: 21338521]
33. Arbeitman MN, Furlong EE, Imam F, Johnson E, Null BH, Baker BS, et al. Gene expression during the life cycle of Drosophila melanogaster. Science. 2002; 297:2270–5. [PubMed: 12351791]
34. Kassen SC, Ramanan V, Montgomery JE, TB C, Liu CG, Vihtelic TS, et al. Time course analysis of gene expression during light-induced photoreceptor cell death and regeneration in albino zebrafish. Dev Neurobiol. 2007; 67:1009–31. [PubMed: 17565703]
35. Kim KH, Yoo HY, Joo KM, Jung Y, Jin J, Kim Y, et al. Time-course analysis of DNA damage response-related genes after in vitro radiation in H460 and H1229 lung cancer cell lines. Experimental & molecular medicine. 43:419–26. [PubMed: 21633183]
36. Storey JD, Xiao W, Leek JT, Tompkins RG, Davis RW. Significance analysis of time course microarray experiments. Proc Natl Acad Sci U S A. 2005; 102:12837–42. [PubMed: 16141318]
37. Han X, Sung WK, Feng L. Identifying differentially expressed genes in time-course microarray experiment without replicate. Journal of bioinformatics and computational biology. 2007; 5:281–96. [PubMed: 17589962]
38. Billups SC, Neville MC, Rudolph M, Porter W, Schedin P. Identifying significant temporal variation in time course microarray data without replicates. BMC bioinformatics. 2009; 10:96. [PubMed: 19323838]
39. Morimoto RI. Regulation of the heat shock transcriptional response: cross talk between a family of heat shock factors, molecular chaperones, and negative regulators. Genes & development. 1998; 12:3788–96. [PubMed: 9869631]
40. Evans TG, Belak Z, Ovsenek N, Krone PH. Heat shock factor 1 is required for constitutive Hsp70 expression and normal lens development in embryonic zebrafish. Comparative biochemistry and physiology Part A, Molecular & integrative physiology. 2007; 146:131–40.
41. Westerfield, M. A guide for the laboratory use of zebrafish (Danio rerio). 4th. Eugene, OR: 2000. The zebrafish book.
42. Barthel LK, Raymond PA. Subcellular localization of alpha-tubulin and opsin mRNA in the goldfish retina using digoxigenin-labeled cRNA probes detected by alkaline phosphatase and HRP histochemistry. J Neurosci Methods. 1993; 50:145–52. [PubMed: 8107495]
43. Stenkamp DL, Frey RA, Prabhudesai SN, Raymond PA. Function for Hedgehog genes in zebrafish retinal development. Dev Biol. 2000; 220:238–52. [PubMed: 10753513]
44. Leek JT, Monsen E, Dabney AR, Storey JD. EDGE: extraction and analysis of differential gene expression. Bioinformatics. 2006; 22:507–8. [PubMed: 16357033]
45. Zheng Q, Wang XJ. GOEAST: a web-based software toolkit for Gene Ontology enrichment analysis. Nucleic acids research. 2008; 36:W358–63. [PubMed: 18487275]

46. Ross PK, Woods CG, Bradford BU, Kosyk O, Gatti DM, Cunningham ML, et al. Time-course comparison of xenobiotic activators of CAR and PPARalpha in mouse liver. Toxicology and applied pharmacology. 2009; 235:199–207. [PubMed: 19136022]
47. Stenkamp DL, Satterfield R, Muhunthan K, Sherpa T, Vihtelic TS, Cameron DA. Age-related cone abnormalities in zebrafish with genetic lesions in sonic hedgehog. Investigative ophthalmology & visual science. 2008; 49:4631–40. [PubMed: 18502998]
48. Nagashima M, Fujikawa C, Mawatari K, Mori Y, Kato S. HSP70, the earliest-induced gene in the zebrafish retina during optic nerve regeneration: its role in cell survival. Neurochemistry international. 2011; 58:888–95. [PubMed: 21338645]
49. Tucker NR, Middleton RC, Le QP, Shelden EA. HSF1 is essential for the resistance of zebrafish eye and brain tissues to hypoxia/reperfusion injury. PloS one. 2011; 6:e22268. [PubMed: 21814572]
50. Nelson SM, Park L, Stenkamp DL. Retinal homeobox 1 is required for retinal neurogenesis and photoreceptor differentiation in embryonic zebrafish. Developmental biology. 2009; 328:24–39. [PubMed: 19210961]
51. Stenkamp DL, Frey RA. Extraretinal and retinal hedgehog signaling sequentially regulate retinal differentiation in zebrafish. Dev Biol. 2003; 258:349–63. [PubMed: 12798293]
52. Stevens CB, Cameron DA, Stenkamp DL. Plasticity of photoreceptor-generating retinal progenitors revealed by prolonged retinoic acid exposure. BMC developmental biology. 11:51. [PubMed: 21878117]
53. Tucker NR, Middleton RC, Le QP, Shelden EA. HSF1 is essential for the resistance of zebrafish eye and brain tissues to hypoxia/reperfusion injury. PloS one. 6:e22268. [PubMed: 21814572]
54. Nasevicius A, Larson J, Ekker SC. Distinct requirements for zebrafish angiogenesis revealed by a VEGF-A morphant. Yeast (Chichester, England). 2000; 17:294–301.
55. Mao L, Shelden EA. Developmentally regulated gene expression of the small heat shock protein Hsp27 in zebrafish embryos. Gene Expr Patterns. 2006; 6:127–33. [PubMed: 16326146]
56. R DCT. A language and environment for statistical computing. R Foundation for statistical computing; Vienna, Austria: 2006.
57. Hu M, Easter SS. Retinal neurogenesis: the formation of the initial central patch of postmitotic cells. Dev Biol. 1999; 207:309–21. [PubMed: 10068465]
58. Mankes RF, Hoffman T, LeFevre R, Bates H, Abraham R. Acute embryopathic effects of ethanol in the Long-Evans rat. Journal of toxicology and environmental health. 1983; 11:583–90. [PubMed: 6620403]
59. Storey JD, Tibshirani R. Statistical methods for identifying differentially expressed genes in DNA microarrays. Methods in molecular biology (Clifton, NJ). 2003; 224:149–57.
60. Nickerson JM, Frey RA, Ciavatta VT, Stenkamp DL. Interphotoreceptor retinoid-binding protein gene structure in tetrapods and teleost fish. Molecular vision. 2006; 12:1565–85. [PubMed: 17200656]
61. Stenkamp DL, Cunningham LL, Raymond PA, Gonzalez-Fernandez F. Novel expression pattern of interphotoreceptor retinoid-binding protein (IRBP) in the adult and developing zebrafish retina and RPE. Molecular vision. 1998; 4:26. [PubMed: 9841935]
62. Cavodeassi F, Carreira-Barbosa F, Young RM, Concha ML, Allende ML, Houart C, et al. Early stages of zebrafish eye formation require the coordinated activity of Wnt11, Fz5, and the Wnt/beta-catenin pathway. Neuron. 2005; 47:43–56. [PubMed: 15996547]
63. French CR, Erickson T, French DV, Pilgrim DB, Waskiewicz AJ. Gdf6a is required for the initiation of dorsal-ventral retinal patterning and lens development. Dev Biol. 2009; 333:37–47. [PubMed: 19545559]
64. Anckar J, Sistonen L. Heat shock factor 1 as a coordinator of stress and developmental pathways. Advances in experimental medicine and biology. 2007; 594:78–88. [PubMed: 17205677]
65. Davuluri G, Gong W, Yusuff S, Lorent K, Muthumani M, Dolan AC, et al. Mutation of the zebrafish nucleoporin elys sensitizes tissue progenitors to replication stress. PLoS Genet. 2008; 4:e1000240. [PubMed: 18974873]

66. Linney E, Dobbs-McAuliffe B, Sajadi H, Malek RL. Microarray gene expression profiling during the segmentation phase of zebrafish development. Comp Biochem Physiol C Toxicol Pharmacol. 2004; 138:351–62. [PubMed: 15533793]

67. Horne MC, Goolsby GL, Donaldson KL, Tran D, Neubauer M, Wahl AF. Cyclin G1 and cyclin G2 comprise a new family of cyclins with contrasting tissue-specific and cell cycle-regulated expression. J Biol Chem. 1996; 271:6050–61. [PubMed: 8626390]

68. Lele Z, Engel S, Krone PH. hsp47 and hsp70 gene expression is differentially regulated in a stress- and tissue-specific manner in zebrafish embryos. Developmental genetics. 1997; 21:123–33. [PubMed: 9332971]

69. Nagashima M, Fujikawa C, Mawatari K, Mori Y, Kato S. HSP70, the earliest-induced gene in the zebrafish retina during optic nerve regeneration: its role in cell survival. Neurochemistry international. 58:888–95. [PubMed: 21338645]

70. Yeh FL, Hsu LY, Lin BA, Chen CF, Li IC, Tsai SH, et al. Cloning of zebrafish (Danio rerio) heat shock factor 2 (HSF2) and similar patterns of HSF2 and HSF1 mRNA expression in brain tissues. Biochimie. 2006; 88:1983–8. [PubMed: 16938384]

71. Dirks RP, van Geel R, Hensen SM, van Genesen ST, Lubsen NH. Manipulating heat shock factor-1 in Xenopus tadpoles: neuronal tissues are refractory to exogenous expression. PloS one. 2010; 5:e10158. [PubMed: 20405018]

72. Zou Y, Zhu W, Sakamoto M, Qin Y, Akazawa H, Toko H, et al. Heat shock transcription factor 1 protects cardiomyocytes from ischemia/reperfusion injury. Circulation. 2003; 108:3024–30. [PubMed: 14623809]

73. Tetievsky A, Cohen O, Eli-Berchoer L, Gerstenblith G, Stern MD, Wapinski I, et al. Physiological and molecular evidence of heat acclimation memory: a lesson from thermal responses and ischemic cross-tolerance in the heart. Physiol Genomics. 2008; 34:78–87. [PubMed: 18430807]

74. Adachi M, Liu Y, Fujii K, Calderwood SK, Nakai A, Imai K, et al. Oxidative stress impairs the heat stress response and delays unfolded protein recovery. PloS one. 2009; 4:e7719. [PubMed: 19936221]

75. McCormick PH, Chen G, Tlerney S, Kelly CJ, Bouchier-Hayes DJ. Clinically relevant thermal preconditioning attenuates ischemia-reperfusion injury. The Journal of surgical research. 2003; 109:24–30. [PubMed: 12591231]

76. Duester G. A hypothetical mechanism for fetal alcohol syndrome involving ethanol inhibition of retinoic acid synthesis at the alcohol dehydrogenase step. Alcohol Clin Exp Res. 1991; 15:568–72. [PubMed: 1877746]

77. Molotkov A, Duester G. Retinol/ethanol drug interaction during acute alcohol intoxication in mice involves inhibition of retinol metabolism to retinoic acid by alcohol dehydrogenase. J Biol Chem. 2002; 277:22553–7. [PubMed: 11960985]

78. Duester G. Alcohol dehydrogenase as a critical mediator of retinoic acid synthesis from vitamin A in the mouse embryo. The Journal of nutrition. 1998; 128:459S–62S. [PubMed: 9478048]

79. Yelin R, Kot H, Yelin D, Fainsod A. Early molecular effects of ethanol during vertebrate embryogenesis. Differentiation; research in biological diversity. 2007; 75:393–403.

80. Twal WO, Zile MH. Retinoic acid reverses ethanol-induced cardiovascular abnormalities in quail embryos. Alcohol Clin Exp Res. 1997; 21:1137–43. [PubMed: 9309328]

81. Guy RK. Inhibition of sonic hedgehog autoprocessing in cultured mammalian cells by sterol deprivation. Proc Natl Acad Sci U S A. 2000; 97:7307–12. [PubMed: 10860995]

82. Lewohl JM, Wang L, Miles MF, Zhang L, Dodd PR, Harris RA. Gene expression in human alcoholism: microarray analysis of frontal cortex. Alcohol Clin Exp Res. 2000; 24:1873–82. [PubMed: 11141048]

83. Gutala R, Wang J, Kadapakkam S, Hwang Y, Ticku M, Li MD. Microarray analysis of ethanol-treated cortical neurons reveals disruption of genes related to the ubiquitin-proteasome pathway and protein synthesis. Alcohol Clin Exp Res. 2004; 28:1779–88. [PubMed: 15608593]

84. Worst TJ, Tan JC, Robertson DJ, Freeman WM, Hyytia P, Kiianmaa K, et al. Transcriptome analysis of frontal cortex in alcohol-preferring and nonpreferring rats. Journal of neuroscience research. 2005; 80:529–38. [PubMed: 15846778]

85. Pignataro L, Miller AN, Ma L, Midha S, Protiva P, Herrera DG, et al. Alcohol regulates gene expression in neurons via activation of heat shock factor 1. The Journal of neuroscience : the official journal of the Society for Neuroscience. 2007; 27:12957–66. [PubMed: 18032669]
86. Worst TJ, Vrana KE. Alcohol and gene expression in the central nervous system. Alcohol Alcohol. 2005; 40:63–75. [PubMed: 15569717]
87. Evans TG, Yamamoto Y, Jeffery WR, Krone PH. Zebrafish Hsp70 is required for embryonic lens formation. Cell Stress Chaperones. 2005; 10:66–78. [PubMed: 15832949]
88. Shamovsky I, Nudler E. New insights into the mechanism of heat shock response activation. Cellular and molecular life sciences : CMLS. 2008; 65:855–61. [PubMed: 18239856]
89. Silver JT, Noble EG. Regulation of survival gene hsp70. Cell Stress Chaperones. 2012; 17:1–9. [PubMed: 21874533]
90. Fujimoto M, Izu H, Seki K, Fukuda K, Nishida T, Yamada S, et al. HSF4 is required for normal cell growth and differentiation during mouse lens development. The EMBO journal. 2004; 23:4297–306. [PubMed: 15483628]
91. Blechinger SR, Evans TG, Tang PT, Kuwada JY, Warren JT Jr, Krone PH. The heat-inducible zebrafish hsp70 gene is expressed during normal lens development under non-stress conditions. Mechanisms of development. 2002; 112:213–5. [PubMed: 11850198]
92. Gogate SS, Fujita N, Skubutyte R, Shapiro IM, Risbud MV. Tonicity enhancer binding protein (TonEBP) and hypoxia-inducible factor (HIF) coordinate heat shock protein 70 (Hsp70) expression in hypoxic nucleus pulposus cells: role of Hsp70 in HIF-1alpha degradation. Journal of bone and mineral research : the official journal of the American Society for Bone and Mineral Research. 2012; 27:1106–17. [PubMed: 22322648]
93. Ito H, Shimojo T, Fujisaki H, Tamamori M, Ishiyama S, Adachi S, et al. Thermal preconditioning protects rat cardiac muscle cells from doxorubicin-induced apoptosis. Life sciences. 1999; 64:755–61. [PubMed: 10075108]
94. Kelty JD, Noseworthy PA, Feder ME, Robertson RM, Ramirez JM. Thermal preconditioning and heat-shock protein 72 preserve synaptic transmission during thermal stress. The Journal of neuroscience : the official journal of the Society for Neuroscience. 2002; 22:RC193. [PubMed: 11756523]
95. Zhang P, Abraham VS, Kraft KR, Rabchevsky AG, Scheff SW, Swain JA. Hyperthermic preconditioning protects against spinal cord ischemic injury. The Annals of thoracic surgery. 2000; 70:1490–5. [PubMed: 11093475]
96. Chen HW, Hsu C, Lu TS, Wang SJ, Yang RC. Heat shock pretreatment prevents cardiac mitochondrial dysfunction during sepsis. Shock. 2003; 20:274–9. [PubMed: 12923501]
97. Choi YJ, Om JY, Kim NH, Chang JE, Park JH, Kim JY, et al. Heat shock transcription factor-1 suppresses apoptotic cell death and ROS generation in 3-nitropropionic acid-stimulated striatal cells. Molecular and cellular biochemistry. 2013; 375:59–67. [PubMed: 23225230]
98. Kitsantas P, Gaffney KF, Wu H, Kastello JC. Determinants of alcohol cessation, reduction and no reduction during pregnancy. Archives of gynecology and obstetrics. 2013
99. Gonzalez P, Baudrimont M, Boudou A, Bourdineaud JP. Comparative effects of direct cadmium contamination on gene expression in gills, liever, skeletal muscles and brain of the zebrafish (Danio rerio). Biometals. 2006; 19:225–35. [PubMed: 16799861]
100. Linney E, Dobbs-McAuliffe B, Sajadi H, Malek RL. Microarray gene expression profiling during the segmentation phase of zebrafish development. Comparative biochemistry physiolgoy toxicology and pharmacology. 2004; 138:351–62.
101. Lin C, Spikings E, Zhang T, Rawson DM. Effect of chilling and cryopreservation on expression of Pax genes in zebrafish (Danio rerio) embryos and blastomeres. Cryobiology. 2009; 59:42–7. [PubMed: 19397904]

Research Highlights

- We examine eye-specific gene expression in zebrafish embryos exposed to EtOH.
- Components of the cellular stress response were differentially expressed.
- Sub-threshold EtOH plus sub-threshold *hsf1* MO resulted in microphthalmia.
- Upregulation of the stress response partially rescued EtOH-induced microphthalmia.
- Reduced Hsf-1 may mediate the microphthalmic effects of EtOH.

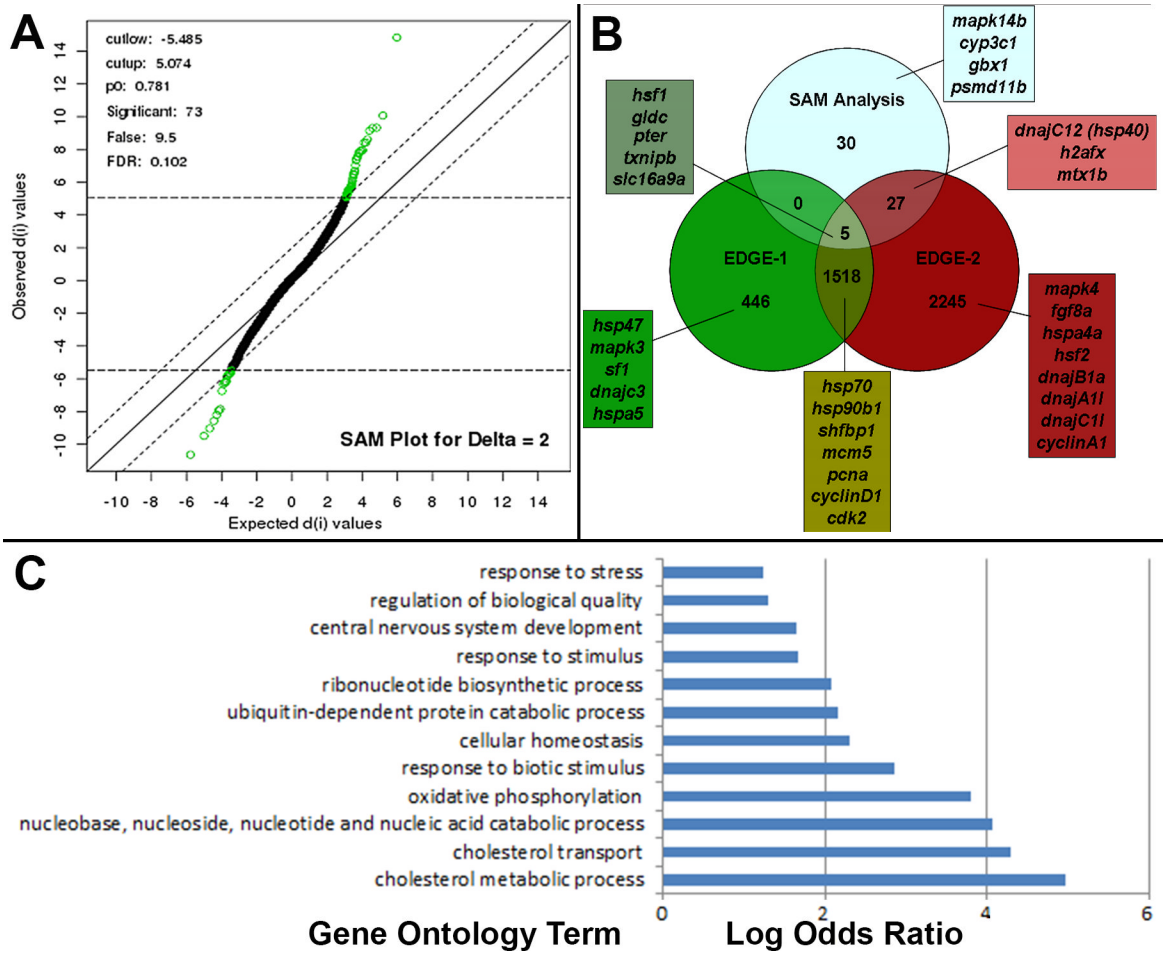

Figure 1. Analyses of microarray results

A. SAM plot representing genes differentially expressed in eyes of ethanol-treated embryos. The genes differentially expressed at significant levels are shown in green and the remaining unperturbed genes are shown in black. The delta (measure of strength of relationship between gene expression and response variable) was set to support a false discovery rate of 0.102. Genes with expression levels that are statistically beyond delta in either direction are plotted either above (up-regulated) or below (down-regulated) the control group. Genes with expression levels that did not change more than the set delta in either direction were considered to be not statistically significantly different at the set false discovery rate. B. Venn diagram showing differentially expressed genes identified by three different approaches for microarray analysis in the untreated vs. ethanol-treated zebrafish embryo eyes. Heat shock response related genes were present in lists derived from SAM analysis and both EDGE analyses (*hsp-40*, *hsf-1*, *hsbp-1*). C. Differentially expressed genes identified by the EDGE2 analysis were classified into selected biological processes using GOEAST.

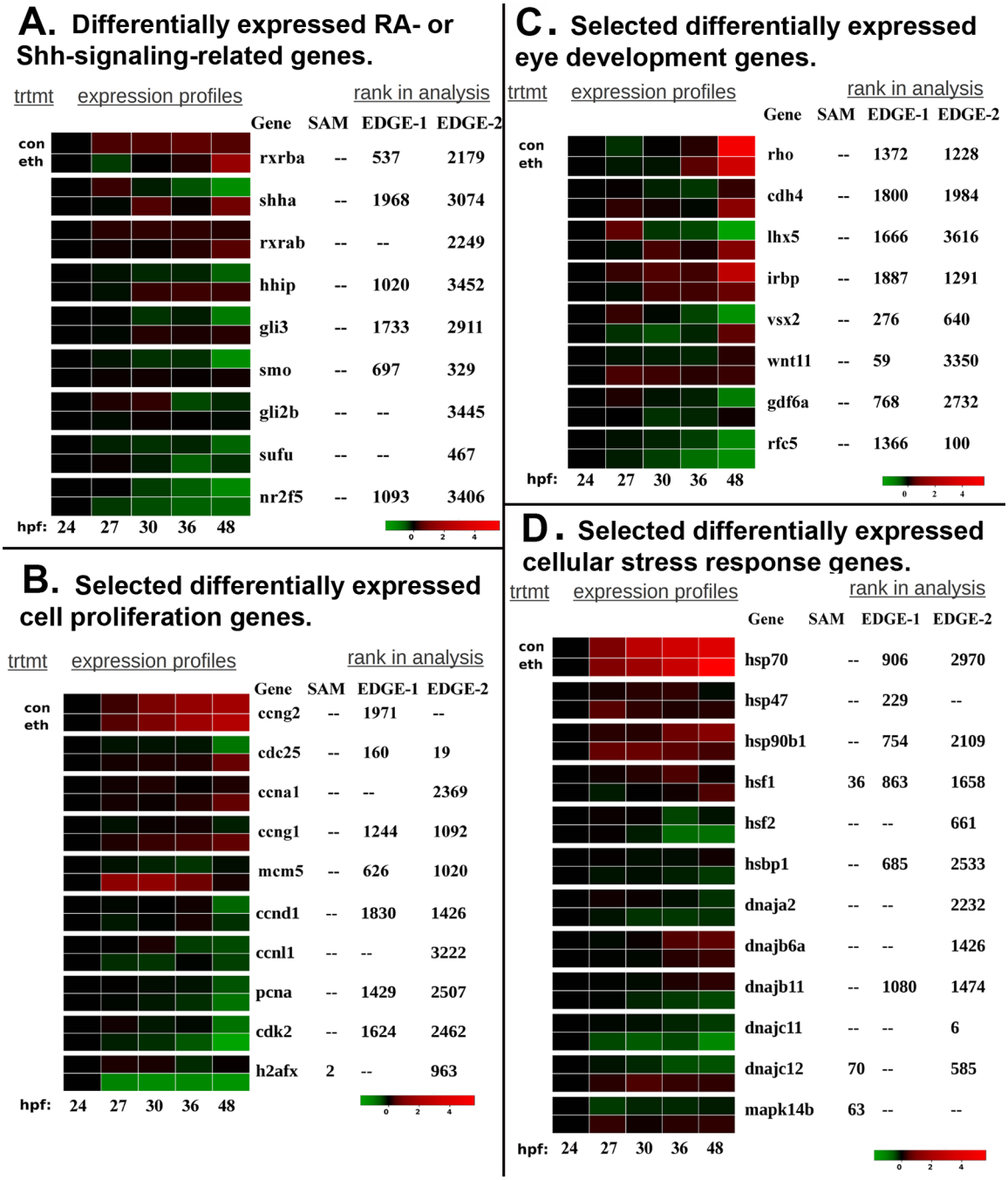

Figure 2. Heatmaps of selected genes that are differentially expressed in ethanol-treated eyes, according to SAM or EDGE analyses

A. Genes related to RA signaling or Shh signaling, identified as differentially expressed according to SAM (10% FDR), EDGE-1 or EDGE-2 (0.05 q cut-off). Rank in analysis is according to statistical significance. B-D. Selected genes related to cell proliferation (B), eye development (C), and the cellular stress response (D), identified as differentially expressed according to SAM (10% FDR), EDGE-1 or EDGE-2 (0.05 q cut-off). Rank in analysis is according to statistical significance. Con, control; eth, ethanol; hpf, hours post-fertilization; green, reduced as compared to 24 hpf control; red, increased as compared to 24 hpf control; black, matching that of 24 hpf control (= 0 in the scales).

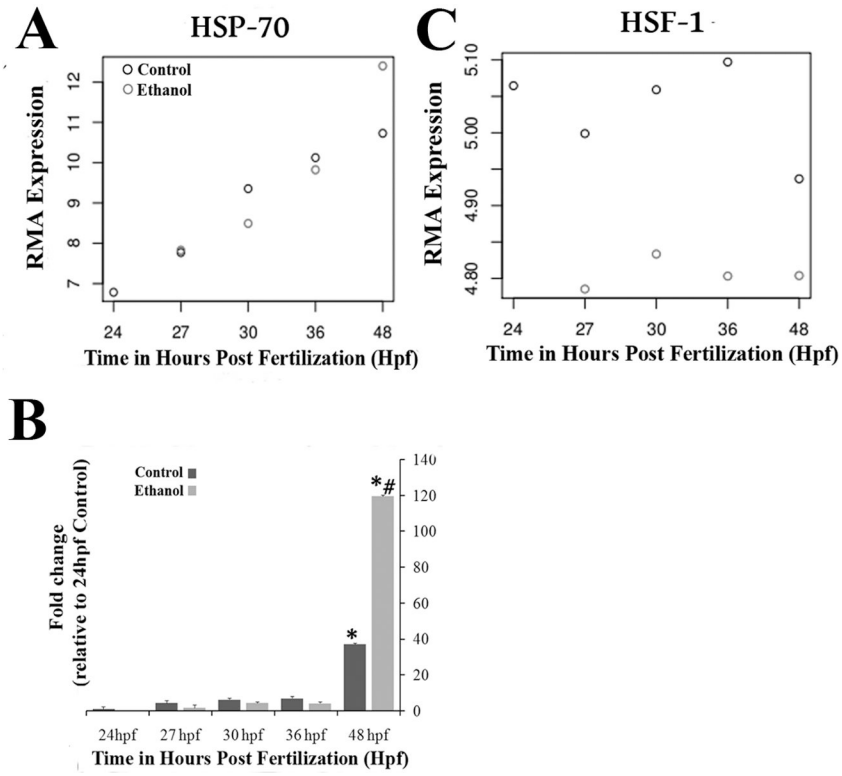

Figure 3. *Hsp-70* and *hsf-1* expression in ethanol-treated eyes

Time-series microarray results for *hsp-70* (A) and *hsf-1* (C) in eyes following ethanol exposure during retinal neurogenesis, expressed as RMA expression levels and represented as dot plots (limits of y-axes selected to minimize white space). The bar graph (B) shows relative expression *of hsp-70* determined using qRT PCR with β-actin as the endogenous control in eye-specific material. Fold changes in expression level are relative to the level at 24 hpf, error bars represent std. error of mean. Asterisk (*) represents significant change in expression of groups compared to 24 hpf control ($p < 0.05$), number sign (#) represents significant difference as compared to control at same sampling time ($p < 0.05$).

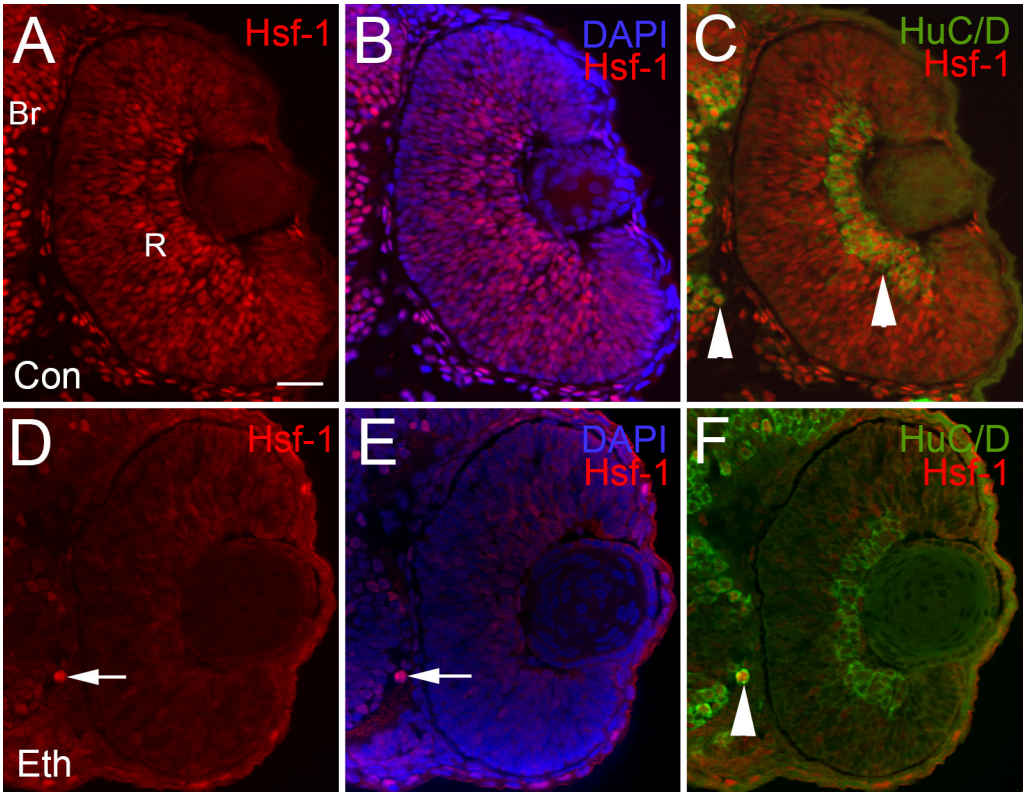

Figure 4. Hsf-1 protein distribution in control and ethanol-treated embryos at 36 hpf

Sections derived from control (A-C) or ethanol-treated embryos (D-F), were processed for indirect immunofluorescence using an anti-Hsf-1 antibody. A and D show Hsf-1 labeling only; note Hsf-1-positive cells in brain (Br) and retina (R) of control embryo, and only a few Hsf-1-positive cells in brain of ethanol-treated embryo (arrow) and none in retina. B and E show Hsf-1 labeling and DAPI counterstain to label nuclei. C and F show Hsf-1 label together with HuC/D, a neuronal marker; arrowheads show colabeled cells. Scale bar = 25 μm.

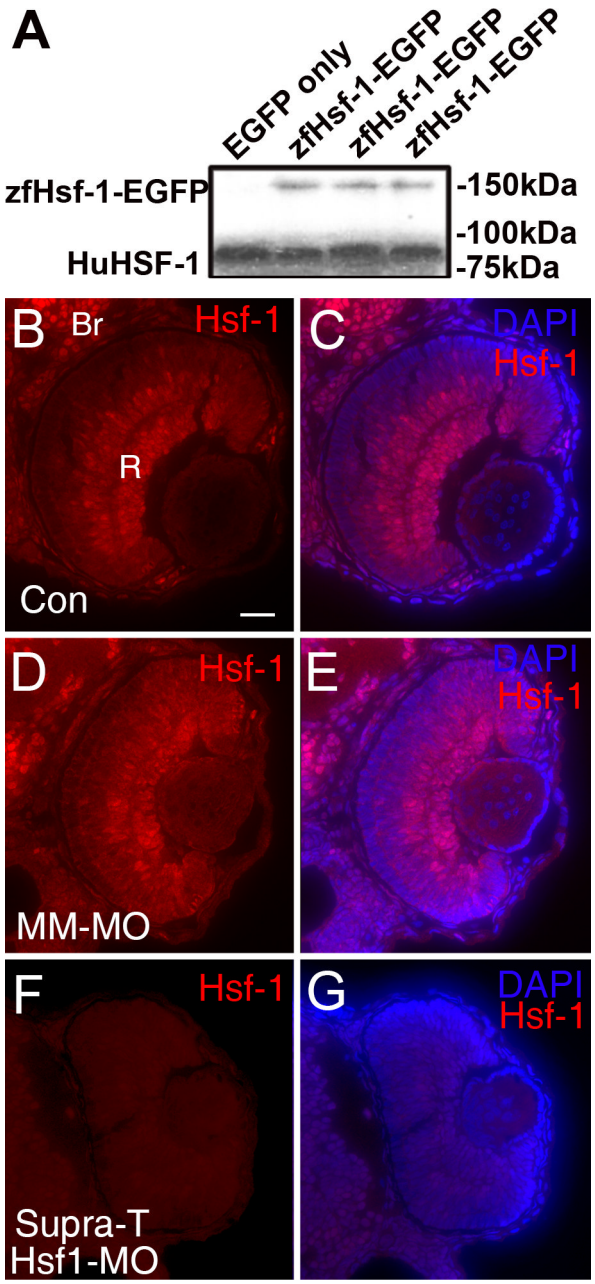

Figure 5. Characterization of Hsf-1 antibody

A. Western blot of HeLa cell protein using the anti-human Hsf-1 antibody from Thermo-Scientific. A prominent band is seen at the predicted molecular weight of human HSF-1 (HuHSF-1) in all lanes. An additional, higher molecular-weight band is seen in extracts of HeLa cells transfected with a plasmid encoding zebrafish Hsf-1-EGFP fusion protein (zfHsf-1-EGFP). B-G. Loss of Hsf-1 immunoreactivity in tissues of *hsf-1* morphant embryos. Sections derived from control embryos (B-C), embryos treated with a control morpholino (MM-MO; D-E), or *hsf-1* morphants (supra-t *hsf-1* MO; F-G), fixed at 48 hpf, were processed for indirect immunofluorescence using the anti-Hsf-1 antibody [48]. B, D, and F show Hsf-1 labeling only; note immunopositive cells in brain (Br) and retina (R) of control embryo, and no immunopositive cells in brain or retina of *hsf-1* morphant. C, E, and G show Hsf-1 labeling together with DAPI counterstain to label nuclei. Scale bar = 25 μm.

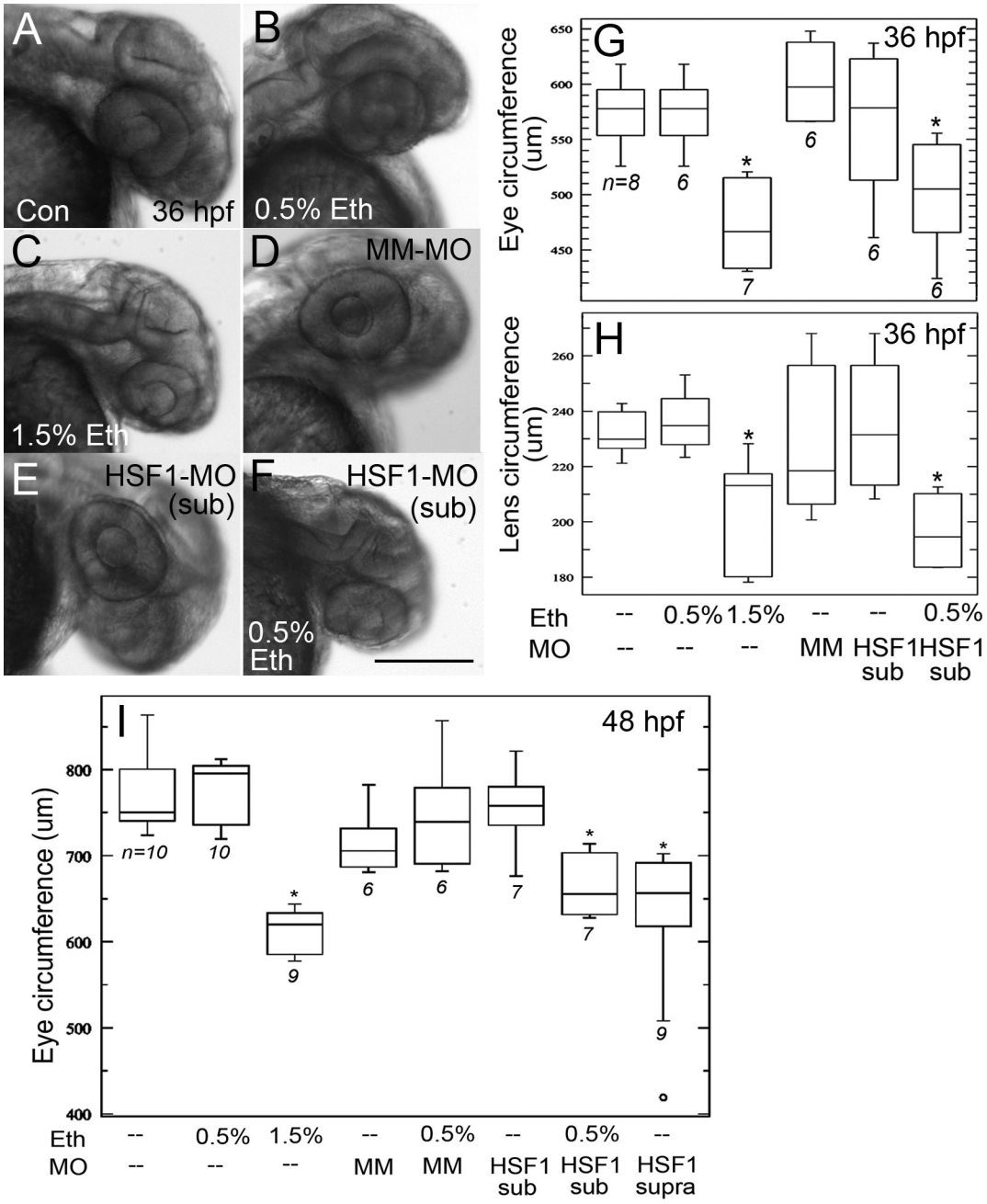

Figure 6.

Sub-threshold ethanol treatment combined with sub-threshold *hsf-1* MO-mediated knockdown results in microphthalmia. A.-H. Embryos were fixed at 36 hpf following no treatment (A), treatment with 0.5% ethanol at 24 hpf (B), treatment with 1.5% ethanol at 24 hpf (C), treatment with a control MO (MM-MO) at the 1-2-cell stage (D), sub-threshold *hsf-1* MO at the 1-2-cell stage (E), and combined sub-threshold *hsf-1* MO and 0.5% ethanol (F). G-H. Eye circumference (G) and lens circumference (H) measurements at 36 hpf; in the boxplots, the boxes demarcate the 25th and 75th percentiles, dark horizontal lines designate the medians, whiskers represent the upper and lower limits, and any open circles indicate outliers. Asterisks (*) appear above groups that are significantly different from the control groups (p value<0.05; ANOVA, post hoc analysis). Numbers of embryos in each group (n)

are provided below each boxplot (“n”s for H are the same as those for G). Limits of y-axes were selected to minimize white space. I. Eye circumference measurements from a separate experiment in which embryos were fixed at 48 hpf. Scale bar in A (applies to all images) = 250 μm.

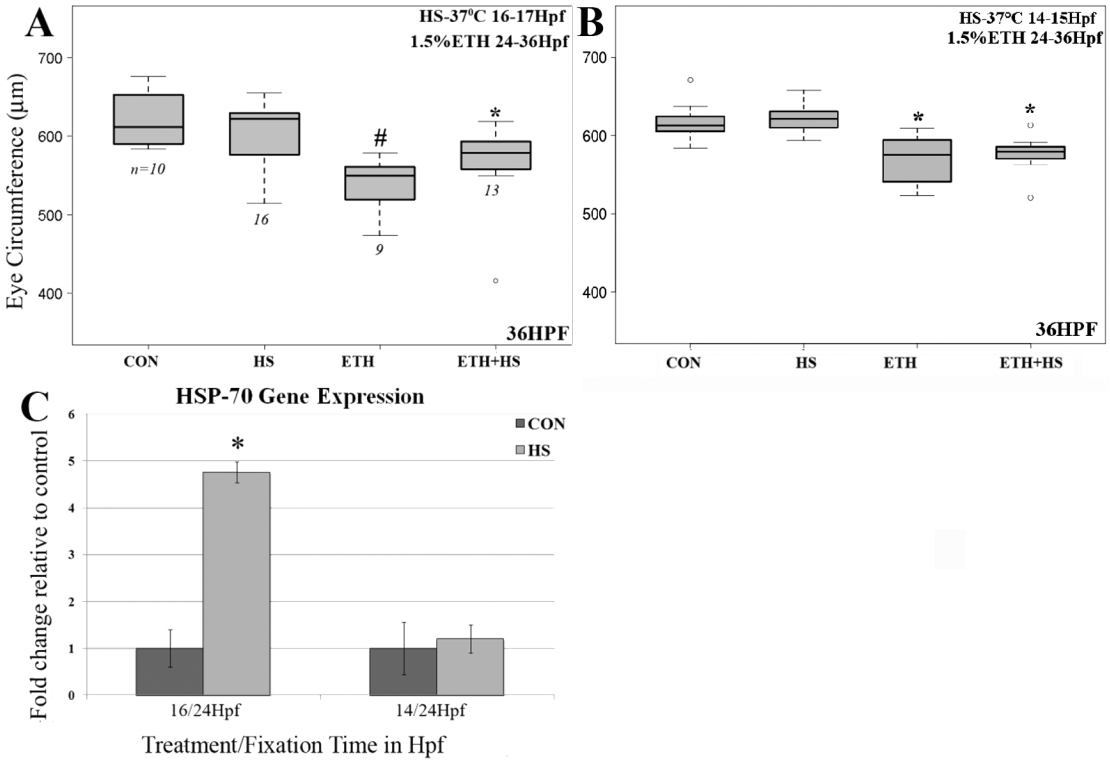

Figure 7. Ethanol-induced microphthalmia is partially prevented by a thermal preconditioning protocol that up-regulates *hsp-70*

A, B. Eye circumference measurements following thermal preconditioning (37°C) for 1 hour beginning at 16 hpf (A) or 14 hpf (B), followed by exposure to 1.5% ethanol at 24 hpf. Embryos were fixed for eye measurements at 36 hpf. Boxplots were generated in R statistical software; the boxes demarcate the 25th and 75th percentiles, dark horizontal lines designate the medians, whiskers represent the upper and lower limits, and the open circles indicate outliers. Asterisks (*) appear above groups that are significantly different from control, number signs (#) appear above groups that are significantly different from both control and HS (heat shock) groups (p value<0.05; ANOVA, post hoc analysis). Numbers of embryos in each group (n) are provided below each boxplot. B. Relative expression of *hsp-70* mRNA determined using qRT PCR with β-actin as the endogenous control, in total RNA from control and following thermal preconditioning (37°C) at 14 hpf or 16 hpf for 1 hour, with embryos collected at 24 hpf. Fold changes in expression level are relative to the level of respective controls, error bars represent std. error of mean. Asterisks (*) represents significant change in expression of groups compared to control (p <0.05, T-test).

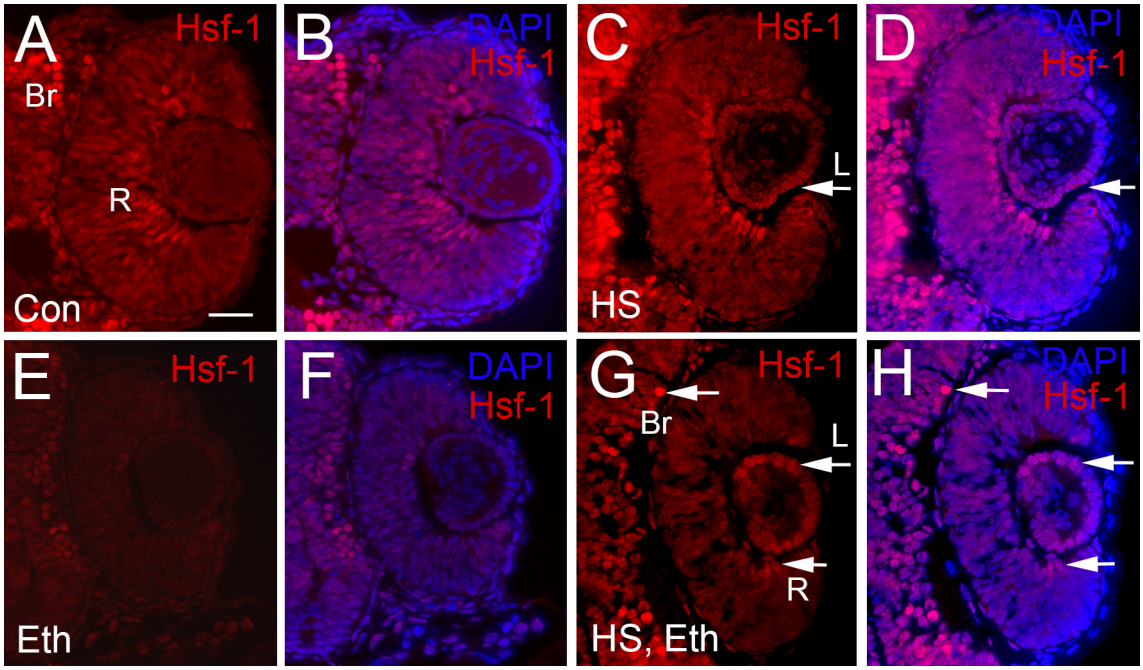

Figure 8. Hsf-1 protein distribution following thermal preconditioning

Embryos were fixed at 36 hpf and processed as cryosections for indirect immunofluorescence with an anti-Hsf antibody. A, B. Untreated (Con) embryo, with Hsf-1-positive cells in brain (Br) and retina (R); B shows Hsf-1 immunofluorescence along with nuclear DAPI (blue) staining. C, D. Embryo subjected to thermal preconditioning (heat shock; HS) at 16 hpf, with Hsf-1-positive cells now also present in lens epithelium (L); D shows Hsf-1 immunofluorescence along with DAPI. E, F. Embryo treated with 1.5% ethanol at 24 hpf (Eth); F includes DAPI counterstain. G, H. Embryo subjected to thermal preconditioning at 16 hpf and treated with ethanol at 24 hpf (HS, Eth). Note maintenance of Hsf-1 expression in brain (Br), retinal cells (R), and appearance of Hsf-1-positive cells in lens epithelial cells (L); H shows Hsf-1 immunofluorescence along with DAPI. Scale bar = 25 μm.